Work of cavity formation inside a fluid using free-energy perturbation theory

Sudeep Punnathanam and David S. Corti*
School of Chemical Engineering, Purdue University, West Lafayette, Indiana 47907-2100, USA
(Received 6 September 2003; published 10 March 2004)

A semiempirical approach, based on both the scaled particle theory of hard particle fluids and free-energy perturbation methods, that predicts the work of formation of a cavity inside a model fluid is presented. The method is tested using the pure component Lennard-Jones fluid. A good agreement between values obtained via the theory and molecular simulation is observed even as the size of the cavity becomes larger than the effective diameter of Lennard-Jones particles. The method also yields reasonably accurate estimates when the pressure of the liquid is quite low, which is the case for liquids close to the coexistence line, or when the pressure is negative, which is the case when the liquid is metastable.

DOI: 10.1103/PhysRevE.69.036105 PACS number(s): 05.70.Ce, 05.20.Jj

I. INTRODUCTION

Work of cavity formation inside a solvent is an important term contributing to the solvation free energy of a solute particle. Hence, knowledge of the work of cavity formation is essential when predicting the free energy of formation of various structures such as colloids, vapor bubbles, etc., inside a solvent liquid. For example, the interaction between apolar solutes and water is characterized by the hydrophobic effect. These apolar solutes are usually modeled as hard spheres [1], and so become equivalent to cavities placed within the waterlike solvent. A proper understanding of the hydrophobic effect requires accurate predictions of the solvation free energies of these cavities in water.

The most widely used theory for predicting the work of cavity formation in a fluid is the scaled particle theory (SPT) developed by Reiss *et al.* [2]. SPT, in the original developments, predicts the work of cavity formation inside a fluid comprised of hard particles. Within SPT, an interpolation scheme is devised that connects the exact expressions for cavity formation in the small cavity limit and in the limit of cavities of macroscopic size. SPT is quite successful in predicting the work of cavity formation within hard particle fluids, even for large cavities and over a wide range of bulk densities. This has motivated many researchers to use the formalism of SPT to develop expressions for the work of cavity formation in fluids with attractive potentials and without hard cores, such as the Lennard-Jones fluid. One of the earlier attempts to modify SPT was by Pierotti [3]. He developed a semiempirical approach in which the value of the pressure used in the equations of SPT was replaced by one obtained either experimentally or by molecular simulation. The method was quite successful in predicting the work of formation for small cavities. For the case of liquids close to the coexistence line, the method was able to predict a drying transition [4] at large cavity sizes, which is a lowering of the local density near the cavity surface below that of the bulk density. Later, Stillinger [5] improved upon this approach to include the variance of density fluctuations within small volumes. As shown later in the paper, the performance of SPT with these modifications, however, suffers when the size of the cavity becomes larger than the particle diameter, especially when the fluid is near the liquid coexistence line where the pressures are quite low or in the metastable liquid region where one encounters negative pressures. This conclusion was also noted by Henderson [6].

A recent theory proposed by Lum, Chandler, and Weeks [1] (LCW) was shown to be able to overcome some of these difficulties. The theory uses a mean-field integral equation along with a linear response theory recently developed by Weeks and co-workers [7]. The LCW theory requires that a set of integrodifferential equations be solved by iteration to obtain the density profile around the cavity. Huang and Chandler [4] applied the LCW theory to predict the work of cavity formation in a Lennard-Jones liquid. They were able to obtain accurate values of the works of formation of cavities with sizes approaching nearly three times the effective diameter of a Lennard-Jones particle, even when the liquid was close to the coexistence line. Later Katsov and Weeks (KW) [8] calculated the work of formation of the cavity for the same conditions as those given by Huang and Chandler [4] with fewer approximations as compared to the LCW theory. Although good estimates are obtained, both these approaches require a fair amount of computational effort, particularly if large cavity sizes are to be studied.

In an attempt to lessen the computational effort needed to generate works of cavity formation over a broad range of cavity sizes and fluid properties, we propose an alternative method that is based on an extension of the SPT equations via the application of the free-energy perturbation theory for liquids developed by Weeks, Chandler, and Andersen [9]. As mentioned earlier, SPT gives an expression for the work of cavity formation inside a hard sphere fluid. In the perturbation theory approach, the liquid is treated as a system of particles governed mainly by the repulsive part of the intermolecular potential with the attractive part of the potential acting as a small perturbation. The fluid interacting only through the repulsive potential is considered as the reference system. For practical calculations, the reference fluid is then mapped onto an equivalent hard sphere fluid. Hence, it seems natural to consider an approach that combines elements of both SPT and the free-energy perturbation theory to predict

*Author to whom correspondence should be addressed. Electronic address: dscorti@ecn.purdue.edu

the work of cavity formation inside a fluid with an attractive potential. This is precisely the approach we develop and discuss in this paper.

The remainder of the paper is structured as follows. In Sec. II, we describe our method for predicting the work of cavity formation in fluids with attractive potentials. In Sec. III, we test the predictions of our approach against the results obtained from Monte Carlo simulations of a Lennard-Jones liquid. A comparison of our predictions with those generated by other existing approaches is also made in this section. Conclusions are presented in Sec. IV.

II. THEORY

Consider a system of N particles in a macroscopic volume V and at a temperature T containing a spherical cavity of radius λ. A cavity is defined as a spherical region inside the fluid that is devoid of any centers of the particles comprising the fluid. Let ρ_b denote the bulk fluid density and P the pressure of the fluid. Without loss of generality, the volume V is assumed to be spherical in shape having a radius R with its center matching the center of the cavity ($R \gg \lambda$). The N particles interact with each other through a pairwise additive potential given by u. The pair potential is divided into two parts, namely, u_0 which is comprised of the steep repulsive part and u_1 which comprises the remaining weak attractive part. Let A be the Helmholtz free energy of the fluid containing the cavity. With the potential decomposed into two parts, we have [10]

$$A = A_0 + A_1 + O(\beta), \tag{1}$$

where A_0 is the Helmholtz free energy of the reference system that consists of particles interacting with a potential of u_0 only, A_1 is the first-order contribution to the free energy due to the attractive potential u_1, and $\beta = 1/(kT)$ with k being the Boltzmann's constant. It should be noted that both A_0 and A_1 are functions of λ. Following what is known from the perturbation theory of uniform fluids [10], we express A_1 in an analogous manner:

$$A_1(\lambda) = \frac{1}{2}\int\int u_1(|\vec{r}_1 - \vec{r}_2|)\rho_0^{(2)}(\vec{r}_1,\vec{r}_2,\lambda)d\vec{r}_1\, d\vec{r}_2, \tag{2}$$

where $\rho_0^{(2)}(\vec{r}_1,\vec{r}_2,\lambda)d\vec{r}_1 d\vec{r}_2$ is the conditional probability that a particle is at position $\vec{r}_1$ in a volume $d\vec{r}_1$ and another particle is at position $\vec{r}_2$ in a volume $d\vec{r}_2$ inside a liquid comprised of particles interacting with the reference potential u_0 and given a cavity of radius λ at the origin. Equation (2) is formally exact. In its current form, however, Eq. (2) cannot be evaluated since $\rho_0^{(2)}(\vec{r}_1,\vec{r}_2,\lambda)$ is generally not known.

To proceed, we first rewrite $\rho_0^{(2)}(\vec{r}_1,\vec{r}_2,\lambda)$ as

$$\rho_0^{(2)}(\vec{r}_1,\vec{r}_2,\lambda) = \rho_0^{(1)}(\vec{r}_1,\lambda) \times \rho_0^{(1)}(\vec{r}_2,\lambda) \times g_0^{(2)}(\vec{r}_1,\vec{r}_2,\lambda), \tag{3}$$

where $\rho_0^{(1)}(\vec{r},\lambda)$ is the local fluid density of the reference fluid at position $\vec{r}$ given a cavity of radius λ at the origin and $g_0^{(2)}(\vec{r}_1,\vec{r}_2,\lambda)$ is the pair correlation function of the nonuniform reference fluid. Equation (3) is simply a definition of $g_0^{(2)}(\vec{r}_1,\vec{r}_2,\lambda)$. The three terms on the right-hand side of Eq. (3) are still unknown and in order to evaluate them we use the following approximations. We use the mean-field approximation for $\rho_0^{(1)}(\vec{r}_1,\lambda)$ and $\rho_0^{(1)}(\vec{r}_2,\lambda)$, i.e.,

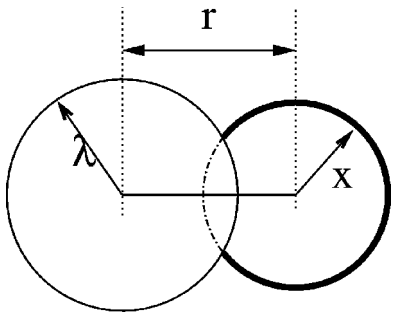

FIG. 1. Two-dimensional view of a cavity of radius λ and a sphere of radius x located at a distance r from the cavity center. The thick solid line is the surface area of the sphere of radius x that is outside the cavity. The function $f(x,r,\lambda)$, as defined in Eq. (6), is the ratio of this surface area that falls outside the cavity to the total surface area of the sphere. Note that r represents the distance to particle 1 from the center of the cavity and x denotes the distance between particles 1 and 2.

$$\rho_0^{(1)}(\vec{r},\lambda) = \begin{cases} 0 & \text{if } |\vec{r}| < \lambda \\ \rho_b & \text{otherwise,} \end{cases} \tag{4}$$

and $g_0^{(2)}(\vec{r}_1,\vec{r}_2,\lambda)$ is replaced by the pair correlation function for a uniform reference fluid, $g_0^{(2)}(\vec{r}_1,\vec{r}_2)$. The net effect of these approximations is that correlations inside the fluid due to the presence of the cavity are completely ignored except for the fact that the density inside the cavity is zero. Despite these simplifications, the approach, developed further below, yields reasonably accurate predictions of the work of cavity formation (see Sec. III).

With our chosen approximations, all terms in Eq. (2) are functions of $\vec{r}_1 - \vec{r}_2$ only. Hence, we can integrate over, say, the position of particle 1 and the vector defining the orientation between particles 1 and 2. Let $\vec{r}_1 \equiv \{r,\theta_1,\phi_1\}$ and $\vec{r}_2 - \vec{r}_1 \equiv \{x,\theta_2,\phi_2\}$, giving us a total of six variables. Due to spherical symmetry we can immediately integrate over variables θ_1 and ϕ_1. The lower and upper limits of the integral over r are λ and R, respectively. Using Eqs. (3) and (4) in Eq. (2), and replacing $g_0^{(2)}(\vec{r}_1,\vec{r}_2,\lambda)$ by $g_0^{(2)}(\vec{r}_1,\vec{r}_2) = g_0(x)$, the limits of the integral over x are functions of r and λ. We can now integrate over the variables θ_2 and ϕ_2 for a given x, but we also need to account for Eq. (4). The integration over θ_2 and ϕ_2 is, however, equivalent to determining the area of a sphere of radius x that lies outside a cavity of radius λ when the center of the two spheres are separated by a distance r (see Fig. 1). In other words, because of Eq. (4), θ_2 and ϕ_2 must be chosen such that particle 2 does not lie inside the cavity. Let $f(x,r,\lambda)$ represent the fraction of the total surface area of the sphere of radius x that is located outside the cavity when the two spheres are separated by a distance r. Therefore, Eq. (2) can now be rewritten as

$$A_1(\lambda)=\frac{\rho_b^2}{2}\int_\lambda^R 4\pi r^2\int_0^\infty 4\pi x^2 f(x,r,\lambda)g_0(x)u_1(x)dx\,dr, \tag{5}$$

where

$$f(x,r,\lambda)=\begin{cases}1 & \text{if } x\leqslant r-\lambda\\ \dfrac{1}{2}+\dfrac{x^2+r^2-\lambda^2}{4xr} & \text{if } r-\lambda<x<r+\lambda\\ 1 & \text{if } r+\lambda\leqslant x\end{cases}. \tag{6}$$

It should be noted that $R\gg\lambda$ in Eq. (5). Also, the upper limit of the inner integral (over x) is formally a function of r and R. The error involved in replacing this upper limit with ∞ (done for convenience) should be inconsequential since we eventually consider differences in A_1. Hence, the properties of the boundary (where $R\gg\lambda$) should be irrelevant.

Now, the work of formation, W, of a cavity of radius λ inside a fluid is the difference between the Helmholtz free energy of a fluid with the cavity, $A(\lambda)$, and that without a cavity, $A(0)$. Using Eq. (1) we can express $W(\lambda)$ as follows:

$$\begin{aligned}W(\lambda)&=A(\lambda)-A(0)=A_0(\lambda)-A_0(0)+A_1(\lambda)-A_1(0)\\&=W_0(\lambda)+W_1(\lambda).\end{aligned} \tag{7}$$

$W_0(\lambda)$ in Eq. (7) is the work of forming of a cavity of radius λ inside the reference fluid. $W_1(\lambda)$ is the contribution to the work of cavity formation due to the attractive part of the potential.

Equation (7) is valid for a closed system, i.e., at constant N,V, and T. Hence, when a cavity is grown inside such a system, the bulk density of the surrounding fluid changes. For a macroscopic system, the change in bulk density is insignificant and hence, the work of cavity formation is well defined for a given state point characterized by T and ρ_b. In other words, W,W_0, and W_1 are intensive variables (in that for large enough systems these variables are independent of the size of the system as long as ρ_b is constant) even though A,A_0, and A_1 are extensive variables (dependent on the system size). In using Eq. (7), the value of the volume V has to be very large so that the same bulk density is obtained for each value of λ. Since A_1 is extensive, the second line of Eq. (7) requires that the difference of two very large quantities $A_1(\lambda)$ and $A_1(0)$ must be calculated. To avoid the numerical errors that result in calculating $W_1(\lambda)$ via $A_1(\lambda)-A_1(0)$, we instead rewrite W_1 as follows:

$$W_1(\lambda)=\int_0^\lambda\left(\frac{\partial A_1}{\partial\lambda}\right)_{N,V,T}d\lambda. \tag{8}$$

In this equation, $(\partial A_1/\partial\lambda)_{N,V,T}$ is an intensive variable (for large enough V), ensuring that the calculated value of W_1 is well behaved as V approaches a large value.

Substituting $\rho_b=N/(V-v_c)$ into Eq. (5), where N is the number of particles, $V(=4\pi R^3/3)$ is the total volume of the system, and $v_c(=4\pi\lambda^3/3)$ is the volume of the cavity, we obtain upon differentiating A_1 with respect to λ that

$$\begin{aligned}\left(\frac{\partial A_1}{\partial\lambda}\right)_{N,V,T}=&\frac{64\pi^3\rho^2\lambda^2}{V-v_c}\int_\lambda^R dr\,r^2\int_0^\infty dx\,x^2 f(x,r,\lambda)g_0(x)u_1(x)+8\pi^2\rho^2\\&\times\int_\lambda^R dr\,r^2\int_0^\infty dx\,x^2\left(\frac{\partial f}{\partial\lambda}\right)_{x,r}g_0(x)u_1(x)-8\pi^2\rho^2\lambda^2\int_0^\infty dx\,x^2 f(x,\lambda,\lambda)g_0(x)u_1(x).\end{aligned} \tag{9}$$

An important approximation used while deriving Eq. (9) is that g_0 is kept constant. In general, a change in λ while keeping N, V, and T constant alters the bulk density of the surrounding fluid, thereby affecting the value of g_0. Also, while evaluating Eq. (9), R has to be sufficiently large such that the values calculated from the obtained integrals correspond to cavity growth within a bulk fluid. In our calculations, the value of R chosen was equal to 100λ.

In order to calculate $W_0(\lambda)$, we map the reference system to a hard sphere fluid of density ρ_b and use an expression for the work of cavity formation within a hard sphere fluid obtained by Matyushov and Ladanyi [11]. Incorporating the more accurate Carnahan-Starling equation of state [12] for hard spheres into the framework of SPT, the work of forming a cavity with radius $\lambda>0.5d$ within a hard sphere fluid, where d is the diameter of the hard sphere particle, is given by [11]

$$\begin{aligned}\beta W_0(\lambda)=&\frac{3\eta}{1-\eta}t+\frac{3\eta(2-\eta)(1+\eta)}{2(1-\eta)^2}t^2\\&+\frac{\eta(1+\eta+\eta^2-\eta^3)}{(1-\eta)^3}t^3-\ln(1-\eta),\end{aligned} \tag{10}$$

where $t=2\lambda/d-1$. For cavities with radii smaller than 0.5σ, the exact relation is used [2]:

$$\beta W_0(\lambda)=-\ln[1-8\eta(\lambda/d)^3]. \tag{11}$$

In the above equations, $\eta\,[=\pi\rho d^3/6]$ is the packing fraction.

As the reference system is mapped onto a hard sphere, an expression for the effective hard sphere diameter of a particle is required. The mapping scheme used for determining the

hard sphere diameter d is described below. The pressure of the fluid, P, with both repulsive and attractive interactions, as given by the van der Waals–type equation, is

$$P = P_0 + 2\pi\rho^2 \int_0^\infty r^2 g_0(r) u_1(r) dr, \tag{12}$$

where P_0 is the pressure of the reference fluid. Normally, P_0 and g_0 are estimated to yield a prediction of P. Here, the values of P and g_0 are assumed to be known *a priori*, possibly from molecular simulations. Hence, P and g_0 are used to evaluate P_0. Then, an appropriate equation of state of a hard sphere fluid is used and a value of d chosen so that the pressure of the hard sphere fluid matches P_0. It should be noted that Eq. (12) is obtained from Eqs. (1) and (2) by differentiating A with respect to V after neglecting the changes in g_0 due to the change in density. We use the accurate Carnahan-Starling [12] equation of state for determining P_0. Finally, with d determined, and W_0 now known, the work of forming a cavity of radius λ is then obtained from Eqs. (7)–(9). This method of determining d is different from the one given by the blip function expansion as used by Weeks, Chandler, and Andersen [9]. This was necessary to get consistent thermodynamics in Eq. (14) which is explained below. The difference between the values of d as obtained from these two methods is, as shown in Sec.III, very small.

Equation (9) can be examined for self-consistency when the cavity approaches macroscopic sizes. We know in the limit of $\lambda \to \infty$, i.e., the cavity becomes a hard wall, that [2]

$$W(\lambda) = \frac{4\pi\lambda^3}{3} P + 4\pi\lambda^2 \gamma_\infty \left(1 - \frac{2\delta}{\lambda}\right) + \cdots, \tag{13}$$

where γ_∞ is the boundary tension between the bulk fluid and a hard wall, and δ is the Tolman length indicating the first-order correction to the boundary tension due to curvature. In other words, Eq. (13) implies that

$$\lim_{\lambda \to \infty} \frac{1}{4\pi\lambda^2} \frac{\partial W}{\partial \lambda} = P. \tag{14}$$

Substitution of Eqs. (7)–(11) into Eq. (14) does in fact lead to Eq. (12), thus satisfying the self-consistency needed for the expression of the work of cavity formation inside a fluid at a pressure P.

III. COMPARISON WITH MOLECULAR SIMULATIONS

In order to evaluate the performance of our method, we compared the predictions from Eqs. (7) to (11) to the work of cavity formation calculated directly from molecular simulations. The reversible work of forming a cavity was calculated via Monte Carlo (MC) simulations within the isobaric-isothermal ensemble. The center of the cavity was kept fixed at the origin, or the center, of the simulation cell. The pressure of the fluid was chosen such that the bulk density of a uniform fluid at the given temperature T is equal to ρ_b. Constant pressure simulations allowed us to maintain a density far away from the cavity surface equal to ρ_b with a smaller number of particles that would have been required in a constant volume simulation.

The work of cavity formation was determined from the following relation [2,13]:

$$W(\lambda) = -kT \ln[\Pr(\lambda)], \tag{15}$$

where $\Pr(\lambda)$ is the probability of successfully inserting a cavity of radius λ at a given point in the fluid. $\Pr(\lambda)$ can be directly calculated from a standard MC simulation, in which the probability of successfully inserting a cavity of size λ is determined. At moderate to high fluid densities, however, the chance of inserting a cavity in which $\lambda > \sigma$ becomes low, and the estimation of $\Pr(\lambda)$ becomes statistically poor. To overcome this problem, an umbrella sampling scheme [14] is employed that favors the formation of large cavities. A cavity of a given size is first introduced into the simulation cell and remains fixed at the center of the cell. In addition to the standard MC displacements of the particles (all particle moves that bring a particle center into the cavity are rejected), another MC trial move is implemented that attempts to change the radius of the cavity while particle positions are held fixed (an attempted increase in λ is rejected if an external particle center is found within the cavity surface). A biasing potential ψ is added to the standard MC sampling scheme to ensure that large cavity sizes are obtained during the simulation. Since the resulting ensemble averages are obtained within the biased simulation, the results must be corrected at the end in order to obtain the ensemble averages for the original, unbiased system. Good statistics for the biased averages will be obtained if $\psi(\lambda) = -W(\lambda)$. Unfortunately, ψ is not known *a priori*. Thus, a series of biased simulations is run for several successive windows in which the cavity radius is restricted to remain within some range, $\Delta\lambda$. The work of insertion is calculated during each window and then curve fitted to a polynomial in λ. This current estimate of the work of cavity formation is extrapolated and used as an estimate for the biasing potential within the next simulation window. The size of the window is then adjusted until a uniform distribution of the cavity radii was obtained, thereby ensuring statistically good estimates of the biased averages. The work curves of each window are finally ''linked'' together by adjusting the value of the constant in the curve fit to obtain the total W versus λ profile.

The number of windows required to obtain W versus λ increases as λ increases. In addition, the range of λ sampled within each simulation window, $\Delta\lambda$, decreased with an increase in λ. Thus, the number of simulation windows rapidly increased as larger cavity sizes were studied. In conjunction with the relatively large system sizes used in this study, the rapid increase in the number of windows prohibited us from determining the work of forming cavities of radii greater than three particle diameters.

Works of cavity formation were obtained for the Lennard-Jones fluid, in which the Lennard-Jones potential u_{LJ} between two particles separated by a distance r is given by

$$u_{\mathrm{LJ}}(r) = 4\epsilon \left[\left(\frac{\sigma}{r}\right)^{12} - \left(\frac{\sigma}{r}\right)^{6} \right], \tag{16}$$

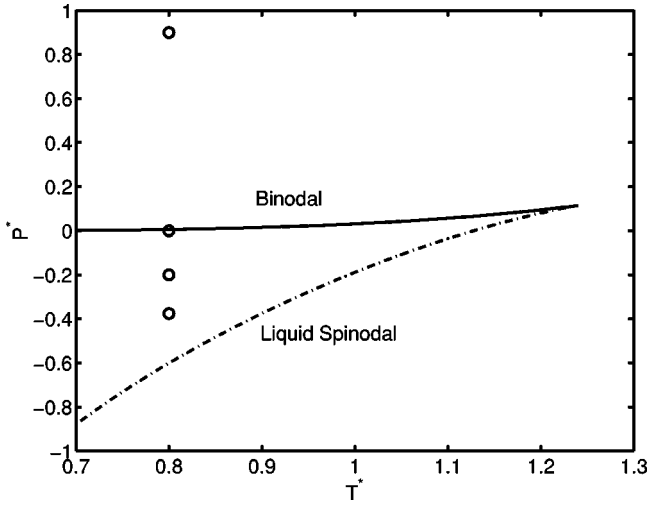

FIG. 2. Pressure-temperature projection of the phase diagram of the Lennard-Jones fluid with the potential truncated and shifted at a distance of 4.0σ. The solid line is the binodal and the dashed-dot line is the liquid spinodal. The lines were calculated from the equation of state given by Johnson *et al.* [15] The circles represent the points at which Monte Carlo simulations were performed to determine the work of cavity formation.

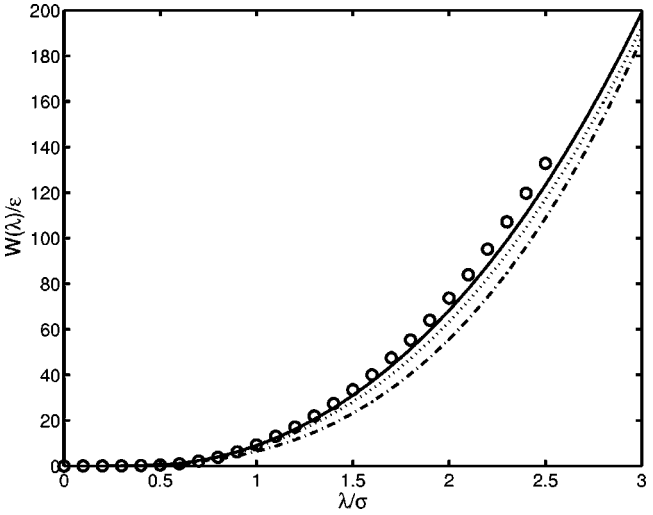

FIG. 3. Work of cavity formation, W, plotted as a function of the cavity radius λ at $T^*=0.8$, $P^*=0.9$. The bulk density ρ_b^* of the fluid is 0.8473. The circles represent calculations from Monte Carlo simulations, the solid line is the prediction from our method, the dotted line is the prediction from Stillinger's method [5], and the dashed-dot line is the prediction from Pierotti's method [3].

where σ is the finite distance at which the potential goes to zero and ϵ is the value of the minima in the Lennard-Jones potential. The potential was also truncated and shifted at a distance of r_c. The truncated and shifted potential eliminated the need to apply long-range corrections. Long-range corrections may be applied only if the density of the fluid is uniform beyond the cutoff radius. Since our simulations contain a cavity, necessarily generating an inhomogeneity within the simulation cell, long-range corrections would not be appropriate. The resulting potential u used for simulation was then equal to

$$u(r)=\begin{cases} u_{\mathrm{LJ}}(r)-u_{\mathrm{LJ}}(r_c) & \text{if } r\leqslant r_c \\ 0 & \text{if } r>r_c. \end{cases} \tag{17}$$

Figure 2 displays the P-T projection of the phase diagram of the Lennard-Jones fluid with the potential given by Eq. (17). The cutoff distance r_c is equal to 4σ. Figure 2 also includes the superheated liquid spinodal. The binodal and the spinodal were obtained from the equation of state of Johnson *et al.* [15]. The critical parameters of this fluid are estimated to be $T_c^*=kT/\epsilon=1.246$,$\rho_c^*=\rho\sigma^3=0.308$, and $P_c^*=P\sigma^3/\epsilon=0.118$. Comparisons between the values of the work of cavity formation as predicted by our method and by molecular simulations were done at a temperature $T^*=0.8$, close to the triple point temperature, and at four separate pressures, namely, $P^*=0.9$ (stable liquid away from the binodal), $P^*=0.0$ (liquid close to coexistence), $P^*=-0.2$ (slightly superheated liquid), and $P^*=-0.3747$ (superheated liquid approaching the spinodal). These state points are also shown in Fig. 2.

In the case of superheated liquids, previous studies [16,17] have shown that there exists an upper limit to the size of a cavity that can be inserted into the liquid. The largest cavity that can be inserted into the metastable liquid is called the critical cavity. Any cavity larger than the critical cavity, when placed inside the superheated liquid, causes an instability that leads to phase separation (i.e., the liquid begins to phase separate towards the vapor phase). This instability, which has been shown to be a true thermodynamic instability [17], prevents us from calculating work profiles for cavities larger than the critical cavity. For $T^*=0.8$ and at pressures $P^*=-0.2$ and $P^*=-0.3757$, the radii of the critical cavities are 6σ and 2.1σ, respectively [16,17]. At $T^*=0.8$ and $P^*=0.0$ the liquid is also superheated (the coexistence pressure is $P_{\mathrm{coex}}^*=6.174\times10^{-3}$ [15]), but the value of the critical cavity is exceedingly large [16,17].

Each simulation consisted of an equilibration period of 10 000 MC cycles (trial moves per particle) followed by a production run of 100 000 MC cycles. The system size of each simulation was at least 3000 particles. The number of particles within the simulation cell for each window was constantly adjusted to ensure that the density profile far from the cavity surface approached the bulk density at least near the edge of the simulation cell. Also, since the interparticle potential was truncated at 4.0σ, an initial simulation box size of twice the sum of the cavity radius and 4.5σ was used. Bulk densities were estimated from the equation of state of Johnson *et al.* [15]. An evaluation of the density profile around the cavity for various cavity sizes revealed that our choice of system size within each window was appropriate.

Figures 3–6 show a comparison of the predictions from our method with those obtained from Monte Carlo simulations. The figures also include the predictions of the suitably modified SPT relations of Peirotti [3] and Stillinger [5]. Both Pierotti's and Stillinger's methods require the specification of an effective hard sphere diameter. We chose this quantity as equal to the maximum distance for which the radial distribution function of the Lenanrd-Jones fluid is essentially equal

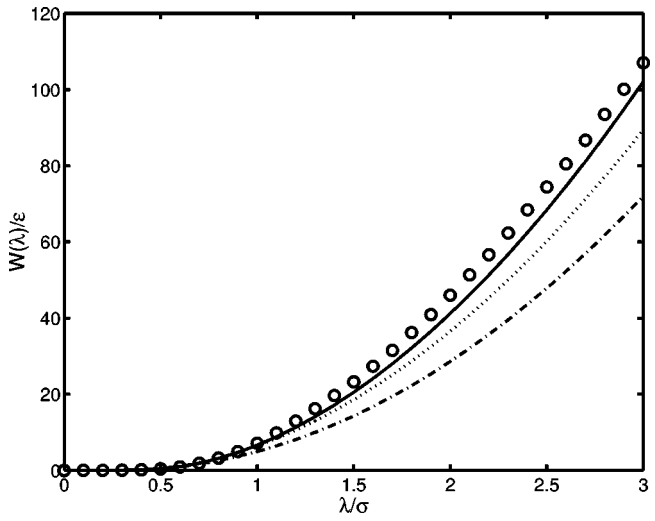

FIG. 4. Work of cavity formation, *W*, plotted as a function of the cavity radius λ at $T^*=0.8$, $P^*=0.0$. The bulk density, ρ_b^*, of the fluid is 0.7803. For an explanation of the symbols and lines see Fig. 3.

to zero. For the range of densities at which the calculations were performed, this quantity remained almost constant and was chosen to be equal to 0.885σ. This criterion was used by Stillinger in his paper when predicting the work of cavity formation inside water. Also, Stillinger's method requires the value of the surface tension of a planar liquid-vapor interface. This value for the temperature $T^*=kT/\epsilon=0.8$, chosen after interpolation from the data given in Holcomb *et al.* [18], was taken to be $0.7\epsilon/\sigma^2$.

In order to use Eq. (9), we divided the potential using the prescription of Weeks, Chandler, and Anderson [9] whereby

$$u_0(r)=\begin{cases} u_{\mathrm{LJ}}(r)+\epsilon & \text{if } r\leqslant 2^{1/6}\sigma \\ 0 & \text{if } 2^{1/6}\sigma<r, \end{cases} \tag{18}$$

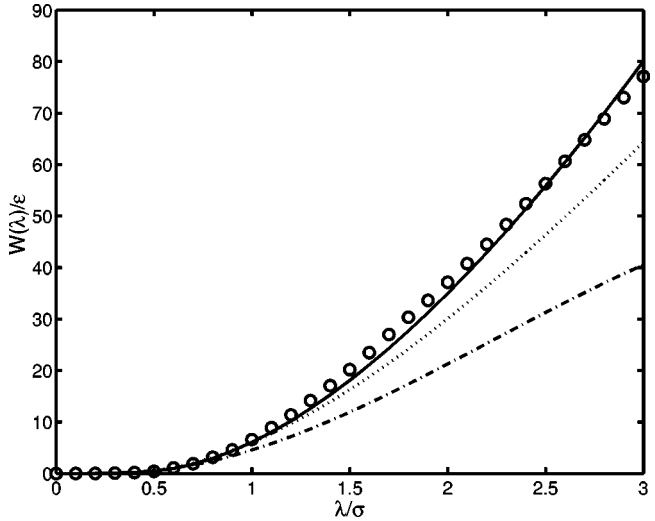

FIG. 5. Work of cavity formation, *W*, plotted as a function of the cavity radius λ at $T^*=0.8$, $P^*=-0.2$. The bulk density ρ_b^* of the fluid is 0.7628. For an explanation of the symbols and lines see Fig. 3.

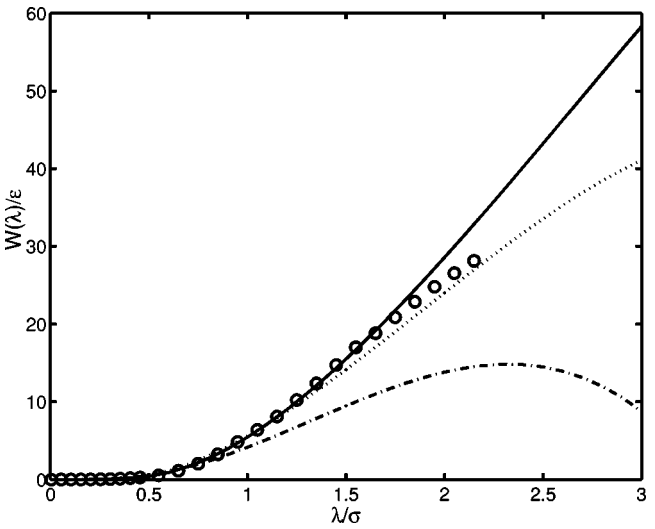

FIG. 6. Work of cavity formation, *W*, plotted as a function of the cavity radius λ at $T^*=0.8$, $P^*=-0.3757$. The bulk density ρ_b^* of the fluid is 0.74. For an explanation of the symbols and lines see Fig. 3.

$$u_1(r)=\begin{cases} -\epsilon-u_{\mathrm{LJ}}(r_c) & \text{if } r\leqslant 2^{1/6}\sigma \\ u_{\mathrm{LJ}}(r)-u_{\mathrm{LJ}}(r_c) & \text{if } 2^{1/6}\sigma<r\leqslant r_c \\ 0 & \text{if } r_c<r. \end{cases} \tag{19}$$

The radial distribution function of the uniform reference fluid, $g_0(x)$, needed to evaluate Eq. (9) and determine an effective hard sphere diameter via Eq. (12) was calculated by Monte Carlo simulations of a uniform fluid interacting via u_0 only. The values of the effective hard sphere diameter, at the various state points for which calculations were performed in this paper, are shown in Table I. The values vary from 0.992σ to 1.005σ. The values of *d* given by the blip function expansion [9] vary from 1.02σ to 1.021σ, which are not very different from our values.

As can be seen from Figs. 3–6, the three methods, on comparison with the simulation results, perform quite well when predicting works of cavity formation for radii less than σ. The predictions of the three methods begin to differ, however, when cavities exceed two to three times the size of the Lennard-Jones particle diameter. On comparison with simulation results, our method consistently outperforms both the Pierotti's and Stillinger's methods. Figure 3 shows the work profile for a cavity inside a stable liquid ($P^*=0.9$) as a

TABLE I. Effective hard sphere diameter *d* of the reference fluid as calculated from Eq. (12) for the various state points discussed in the paper.

T^*	P^*	ρ_b^*	r_c/σ	d/σ
0.8	0.9	0.8473	4.0	1.005
0.8	0.0	0.7803	4.0	1.001
0.8	−0.2	0.7628	4.0	0.998
0.8	−0.3757	0.74	4.0	0.996
0.85	0.022	0.7	2.5	0.992

function of the cavity radius. Although the predictions of the three methods are in a good agreement with values calculated from Monte Carlo simulations, our method provides the closest agreement. When we consider a liquid close to the coexistence line, large differences between the methods begin to develop. For $T^*=0.8$ and $P^*=0.0$ (Fig. 4), the work of cavity formation for a cavity of radius 3σ as calculated from simulations is $\approx 134kT$. Pierotti's and Stillinger's methods underpredict this value by $40kT$ and $20kT$, respectively. Our method predicts a value of $128kT$ which only differs from the simulation result by 4%. Similar trends are observed for the results shown in Fig. 5, which contains the work profiles for a negative pressure liquid ($P^*=-0.2$). This negatively pressured liquid lies in the two-phase region of the liquid-vapor phase diagram and is metastable.

In the case of Fig. 6, which also includes results for a metastable liquid under negative pressure ($P^*=-0.3757$), the predictions from our method match the simulation results quite well up to a cavity of radius 2.1σ. Under these conditions, 2.1σ is the radius of the critical cavity [16,17]. (The current methods are not capable of determining the size of the critical cavity, and so yield predictions beyond the critical cavity.) Our method matches simulation results quite well up to 1.6σ and is certainly more accurate than that of Pierotti. Stillinger's method, however, yields values that are comparable to our method, though this is most likely a fortuitous occurrence (at other negative pressures not far from $P^*=-0.3757$, Stillinger's approach does not match the simulation results as well).

An important point to be noted is that the predictions of Pierotti and Stillinger can be improved by choosing a different value of the effective hard sphere diameter. Nevertheless, the optimized value of the effective hard sphere diameter varies according to the temperature and pressure, and we are unaware of any method to determine this optimized diameter *a priori*.

The eventual appearance of a drying transition about a large enough cavity within a superheated liquid causes the work profile to exhibit a change in curvature as the radius of the cavity approaches the critical size. Each of the three methods presented yields a change in curvature at low and negative pressures, but this is a consequence of the limiting form of W, where the leading order term in Eq. (13) is proportional to the pressure. Each approach is unaware of the limit of stability that appears at the critical cavity. Hence, the changes in curvature exhibited by such methods do not necessarily coincide with the simulation results. Despite this, our method still yields reasonably good estimates of the work profiles at negative pressures.

We also compared the predictions of our method with those from the LCW theory and the method of KW. These results are shown in Fig. 7 for $P^*=0.022$ and $T^*=0.85$. The data for the LCW predictions were obtained from Fig. 2 of Ref. [4] and for the KW predictions were obtained from Fig. 7 of Ref. [8], where the Lennard-Jones potential was truncated and shifted at a distance of 2.5σ. The performance of our approach is comparable to both of these approaches. The LCW predictions are closer to the simulation results at large cavity radii ($\geqslant 2\sigma$). On the other hand, our approach

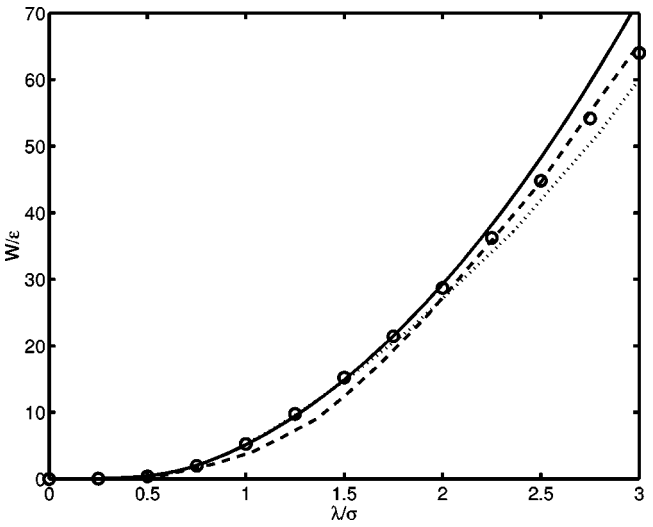

FIG. 7. Comparison of the predictions of the work of cavity formation, W, from our approach (solid line), the LCW [4] theory (dashed line), and the KW approach (dotted line) with the those calculated from Monte Carlo simulations (circles). The data for the LCW theory prediction are taken from Fig. 2 of Ref. [4] and that for the KW approach are taken from Fig. 7 of Ref. [8]. The liquid is at a temperature $T^*=0.85$ and at a pressure $P^*=0.022$. The bulk density of the fluid is $\rho_b^*=0.7$. The Lennard-Jones potential for this calculation has been truncated and shifted at a distance of 2.5σ.

performs better at intermediate cavity radii (between σ and 2σ). The KW approach which is more rigorous than the LCW approach also performs better at intermediate cavity radii but it starts deviating from the simulation results at a smaller radius (1.5σ) as compared to our approach. Although we have not extensively compared the performance of these three approaches, Fig. 7 (along with Figs. 3–6) does indicate that our approach provides a reasonable alternative method to estimating works of cavity formation, even though the amount of rigor incorporated is less than the LCW and the KW approach. In addition, the possibility of improving our method does exist through the incorporation of the higher-order terms of the perturbation expansion in Eq. (5).

We conclude this section by considering the relative magnitudes of W_0, the contribution from the reference system, and W_1, the contribution from the perturbation. Both of these terms contribute to the work of cavity formation, W [see Eq. (7)]. Figure 8 shows a comparison of W_0 and $-W_1$ (W_1 is negative since it is the contribution from the attractive potential). Surprisingly the two terms are of equal order in magnitude, though W_0 is always greater than $-W_1$. In other words, the right-hand side of Eq. (7) is the difference of two large positive numbers. This makes the close agreement between our method and simulation all the more striking, given that in deriving Eq. (9), we have completely ignored the contributions to the free energy due to density correlations arising from the presence of the cavity inside the fluid. In addition, the fluid structure of the reference fluid (purely repulsive potential) in the presence of a cavity is very different from (especially at low and negative pressures) the profiles that develop around a cavity within the Lennard-Jones fluid [7] (comprised of both repulsive and attractive forces). At

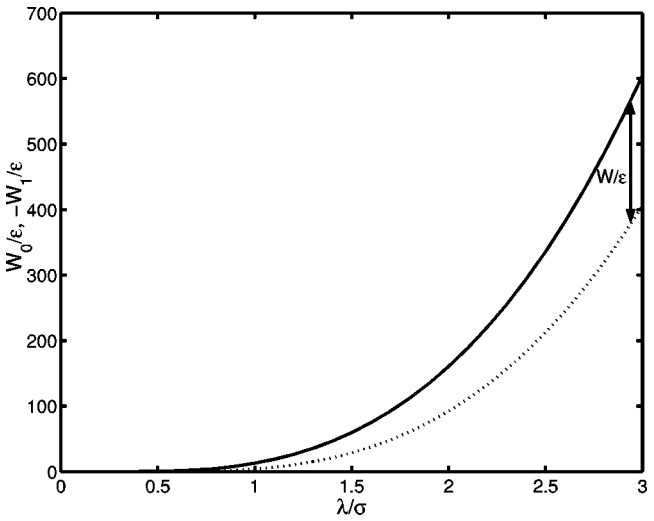

FIG. 8. Comparison of the relative magnitudes of the reference term W_0 and the perturbation term W_1 that both contribute to the total work of cavity formation at $T^*=0.8$ and $P^*=0.9$. The bulk density of the fluid is $\rho_b^*=0.8473$. The solid line represents W_0 and the dotted line represents $-W_1$.

low pressures, for example, the Lennard-Jones fluid exhibits a drying transition when the cavity radii exceed about 1.0σ. The reference fluid, which is similar to a hard sphere fluid in that it consists of steeply repulsive intermolecular forces only, does not produce a drying transition at any cavity size (the local density at the cavity surface always exceeds the bulk density and increases with an increase in the cavity radius, asymptotically at a value of P/kT [2]). The presented work suggests that this difference between the structures that develop around cavities appears to play a minimal role in the predicted values of the work of cavity formation generated by Eqs. (7) and (9), at least up to cavity radii that are three times the diameter of the fluid particles.

IV. CONCLUSIONS

We have presented a semi-empirical method for calculating the work of cavity formation inside a fluid, specifically for fluids that contain an attractive term in their intermolecular potential. The expressions were derived by combining SPT and the free-energy perturbation theory of Weeks, Chandler, and Andersen [9]. For the reference system, we used expressions obtained from SPT. In calculating the perturbation term, we invoked the mean-field approximation, ignoring the density correlations generated inside the fluid due to the presence of the cavity. The predictions of our method matched simulation results quite well, yielding better predictions than the methods of Pierotti [3] and Stillinger [5]. Our method is also comparable to the LCW and the KW methods (at least for the state point considered here), an approach that incorporates more rigor by taking into account the structure of the surrounding fluid. Overall, our method appears to be valid over a broad range of conditions, even performing well when the fluid is metastable. Moreover, although the pressure of the fluid and the radial distribution function for the uniform reference fluid are needed as input, these quantities are straightforward to obtain from molecular simulations.

ACKNOWLEDGMENT

This work was supported by the Shreve Trust of the Purdue Research Foundation.

[1] K. Lum, D. Chandler, and J.D. Weeks, J. Phys. Chem. B **103**, 4570 (1999).
[2] H. Reiss, H.L. Frisch, and J.L. Lebowitz, J. Chem. Phys. **31**, 369 (1959).
[3] R.A. Pierotti, J. Phys. Chem. **69**, 281 (1965).
[4] D.M. Huang and D. Chandler, Phys. Rev. E **61**, 1501 (2000).
[5] F.H. Stillinger, J. Solution Chem. **2**, 141 (1973).
[6] J.R. Henderson, J. Chem. Phys. **116**, 5039 (2002).
[7] J.D. Weeks, K. Katsov, and K. Vollmayr, Phys. Rev. Lett. **81**, 4400 (1998).
[8] K. Katsov and J.D. Weeks, J. Phys. Chem. B **105**, 6738 (2001).
[9] J.D. Weeks, D.C. Chandler, and H.C. Andersen, J. Chem. Phys. **54**, 5237 (1971).
[10] D.A. McQuarrie, *Statistical Mechanics* (Harper & Row, New York, 1976).
[11] D.V. Matyushov and B.M. Ladanyi, J. Chem. Phys. **107**, 5815 (1997).
[12] N.F. Carnahan and K.E. Starling, J. Chem. Phys. **51**, 635 (1969).
[13] H. Reiss, *Statistical Mechanics and Statistical Methods in Theory and Application* (Plenum, New York, 1977).
[14] M.P. Allen and D.J. Tildesley, *Computer Simulation of Liquids* (Oxford Science Publications, Oxford, 1987).
[15] J.K. Johnson, J.A. Zollweg, and K.E. Gubbins, Mol. Phys. **78**, 591 (1993).
[16] S. Punnathanam and D.S. Corti, Ind. Eng. Chem. Res. **41**, 1113 (2002).
[17] S. Punnathanam and D.S. Corti, J. Chem. Phys. **119**, 10224 (2003).
[18] C.D. Holcomb, P. Clancy, S.M. Thompson, and J.A. Zollweg, Fluid Phase Equilib. **75**, 185 (1992).